Hindawi
Geofluids
Volume 2022, Article ID 7365519, 19 pages
https://doi.org/10.1155/2022/7365519

Research Article

Study on the Migration Pattern of Concentrated Brine in Underground Concentrated Brine Storage Reservoir: A Case Study in Ling Xin Mining Area

Xiaolong Hu,[1] Xiaolong Li,[1] Hui Huang,[1] Xidong Song,[1] Jun Gao,[1] Shaoxue Wu,[1] Guocai Kong,[1] and Zhiwei Duan[2]

[1]*Ningxia Coal Industry Company Ling Xin Coal Mine, National Energy Group, Lingwu, Ningxia 751410, China*
[2]*School of Energy and Environmental Engineering, University of Science and Technology Beijing, Beijing 100083, China*

Correspondence should be addressed to Zhiwei Duan; zhiweiduan@xs.ustb.edu.cn

Received 14 December 2021; Accepted 9 April 2022; Published 26 April 2022

Academic Editor: Afshin Davarpanah

The discharge of mine water from underground coal mines in arid areas is leading to extensive water loss and secondary pollution. To eliminate the water loss and environmental pollution, sealing the concentrated brine after the mine water treatment in the underground storage and pumping the clean water to the surface for recycling are effective methods. In this study, focusing on the Ling Xin mining area, China, a coupled model of concentrated brine flow and solute transport in underground reservoir was established. The migration patterns of concentrated brine under two simulation scenarios of long-term penetration and sudden leakage were analyzed. At the same time, it also initially revealed the essence of the environmental pollution caused by the penetration and leakage of the concentrated brine in the underground concentrated brine storage reservoir. Results show that the concentrated brine would penetrate the bottom aquifer in about 60 years in long-term penetration while approximately 40 days in sudden leakage. In addition, the storage time, reservoir permeability, and groundwater head difference were important factors affecting the migration of concentrated brine, where the influence of permeability varieties was the most significant. The results of this study provide technical options for the subsequent study of the environmental risk of underground concentrated brine reservoirs and have important technical significance for the study and engineering application of underground reservoirs in arid areas.

1. Introduction

Northwest China is arid and rainless, and coal mines produce large amounts of mine water during the mining process [1, 2]. Mine water is discharged from the underground to the surface, which causes great loss of water resources, and at the same time, the discharged sewage will affect the surrounding environment to a certain extent [3–5]. As early as the 1970s, the concept of underground reservoirs was put forward. After decades of continuous development of underground reservoir technology, its application in engineering has also been greatly developed. The underground concentrated brine storage reservoir is a kind of underground reservoir, whose principle is to use the coal seam goaf area to form a water storage space with the help of natural coal pillars and artificial dams [6]. This special technology for storing concentrated brine is different from ordinary underground reservoirs in the past, because the special nature of concentrated brine brings many challenges to storage [7]. Although there are many difficulties, it is still a good demonstration for the underground storage of concentrated brine in arid areas.

Ling Xin Mine has installed high-salinity mine water membrane treatment equipment in the mine tunnels. It is used to treat all mine water generated from mining [8]. The treated clean water is discharged to the surface for reuse, and the concentrated brine is sealed in an underground storage [9]. On the one hand, groundwater resources have been effectively used, and the most prominent water shortage problem in arid regions has been alleviated. It reduces the pollution of the surface ecology caused by the discharge of

mine water and at the same time reduces the cost of environmental treatment. On the other hand, the concentrated brine is stored between the goafs of the coal seam, and the porous coal seam can absorb some pollutants and reduce its toxicity [10–13]. However, the concentrated brine in the underground storage will evolve and migrate under long-term storage. How to accurately determine the migration and transformation of concentrated brine in the groundwater environment after it has penetrated or leaked out of the underground storage is full of challenges. Large-scale leakage of high-salinity mine water may affect the quality of groundwater, indirectly affect the surface water system and the surface soil environment, and cause adverse effects such as soil salinization [14–17]. Therefore, it is of great significance to study the migration of concentrated brine in underground storage.

Currently, the research on the migration of pollutants has made great progress [18–20]. González-Quirós and Fernández-Álvarez [21] used numerical simulation to study the pollutant migration caused by the rebound of groundwater in a closed underground coal mine in the Asturias Coal Basin in Spain. Sun et al. [22] studied the impact of the construction of artificial groundwater reservoirs on the groundwater flow and water quality of the reservoir and its downstream and found that the construction of groundwater reservoirs led to the accumulation of nitrate in the storage water. Lin et al. [23] studied the migration of total nitrogen in the riparian buffer zone of agricultural watersheds based on the finite element simulation method and found that the riparian buffer zone had a certain retention effect on soil pollutants. Malinovsky et al. [24] took the Khibiny apatite-nepheline mine in Kola Peninsula, Russia, as an example, collected snow, surface water, and deposited and suspended sediments samples for analysis. The source, migration, and transformation of total dissolved solids and metals in the water area are evaluated. Nico Dalla Libera et al. [25] used a random multicomponent reaction transmission model to calculate the probability that the arsenic concentration in groundwater does not exceed the standard. Shamshad Khan et al. [26] systematically studied the migration behavior of TiO2 nanoparticles in different soil columns and analyzed its influence on the migration rate of copper. However, due to the high degree of complexity of groundwater flow, there are few studies on the migration and transformation of concentrated brine in the groundwater environment [27–30]. Therefore, there is still a vacuum zone for research in this field.

At present, research on underground reservoirs in coal mines also has been gradually gaining attention [31, 32]. Song H et al. [33] established a fluid-solid coupling mathematical model and analyzed the water storage coefficient of the coal mines goaf, which provided a basis for the site selection and construction of concentrated brine underground storage. Yang L et al. [34] established a groundwater reservoir environmental risk assessment model by using the index method and the superposition method, which provided a basis for the quantitative evaluation of groundwater reservoir leakage. Wang Q. [35] studied the formation conditions and mechanism of using underground coal seam goaf to store water and established a series of models related to water storage time. Zhao et al. [36] studied the changes in water quality caused by the removal and transformation of nitrogen and dissolved organic matter during the storage of mine water in underground reservoirs. Kong X et al. [37] studied the depth of artificial dam trenches in underground coal mine reservoirs and found that increasing the trench depth within a certain range can increase the stability of the reservoir. However, research on underground reservoirs is still limited to site selection and construction. There are very few studies on the migration pattern of concentrated brine when it is sealed in underground reservoirs for a long period of time. As a new and special substance, concentrated brine is stored underground, and the possible impact of its migration is not yet known. Whether this impact will affect the safety of the groundwater environment around the underground storage is also urgently needed to be resolved. This study on the migration pattern of concentrated brine in underground storage will make up for these deficiencies.

In this study, the Ling Xin Coal Mine was selected as the research area. Based on a full understanding of local hydrogeological data, a coupled model of concentrated brine flow and solute transport was established, and the migration pattern of concentrated brine under two different simulation scenarios of long-term penetration and sudden leak was analyzed. This research provides technical and data support for the subsequent research on underground concentrated brine storage reservoir, which is of practical significance. At the same time, this article clarifies the direction and extent of the migration of concentrated brine, which effectively reduces the adverse effects of concentrated brine leakage and has certain economic benefits.

2. Materials and Methods

2.1. Study Area and Data. Ling Xin Coal Mine is located in Ling Wu City, Ningxia Hui Autonomous Region. The mine is about 11 km long from north to south, 2.48 km wide from east to west, and has an area of about 27.49 km^2, as shown in Figure 1. In addition, Ling Xin Coal Mine is located in a densely distributed area of mines. The mining area is arid and rainless, the groundwater flows in the northwest direction, and the groundwater quality has a special high salinity background, which is 5610 mg/L.

The underground concentrated brine storage reservoir is located in the northern part of the first mining area, the area where the mining of 14, 15, and 16 coal seams is completed. It occupies a total of 6 working faces: L1614, L1615, L1616, L1814, L1815, and L1816. It is designed to store up to 4,331,300 m^3 of concentrated brine, with a storage life of 4.1 years and the stored concentrated brine with a salinity of 36000 mg/L. The core of the membrane treatment equipment installed in underground mine tunnels is the nanofiltration membrane group, whose function is to remove soluble salts, colloids, organic matter, and microorganisms in the mine water. Its designed processing scale is 500 m^3/h, the product water recovery rate is 85%, and the product water salinity is not more than 500 mg/L. The treated mine

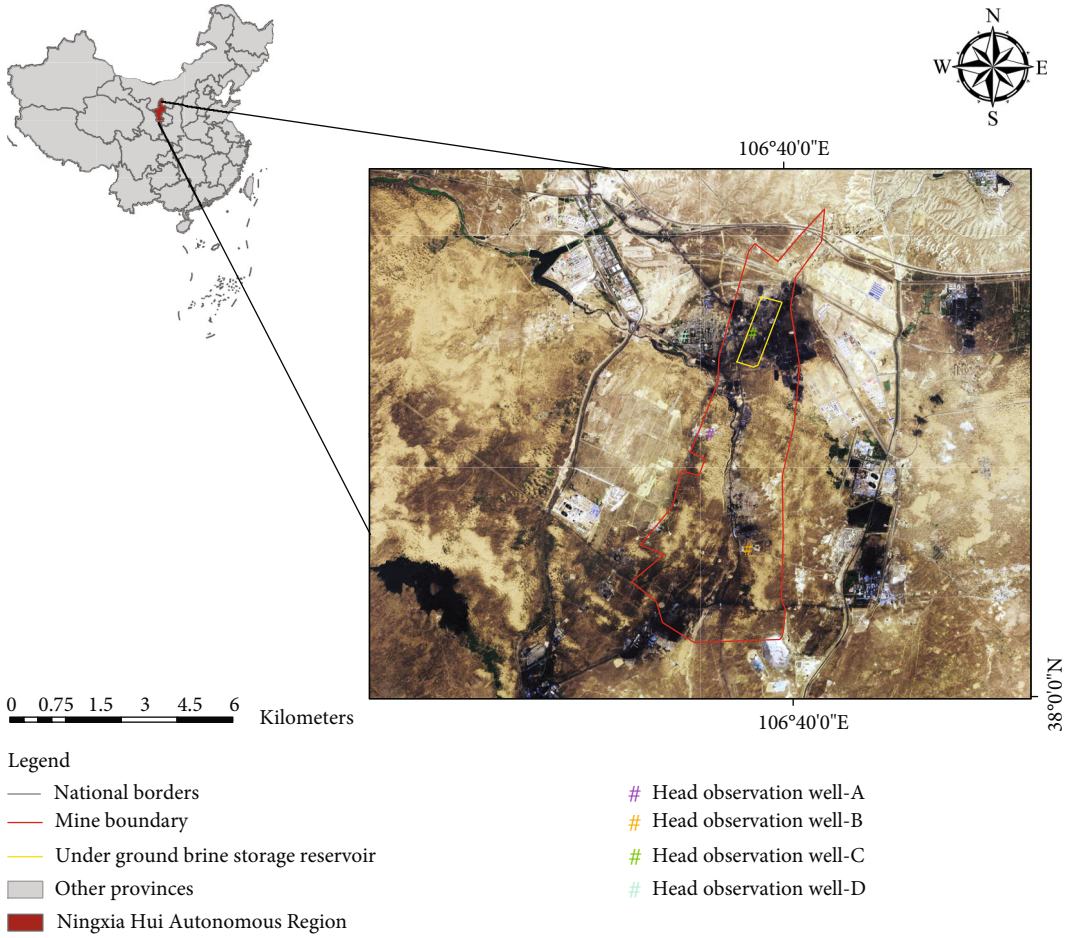

Figure 1: Scope of Ling Xin Coal Mine.

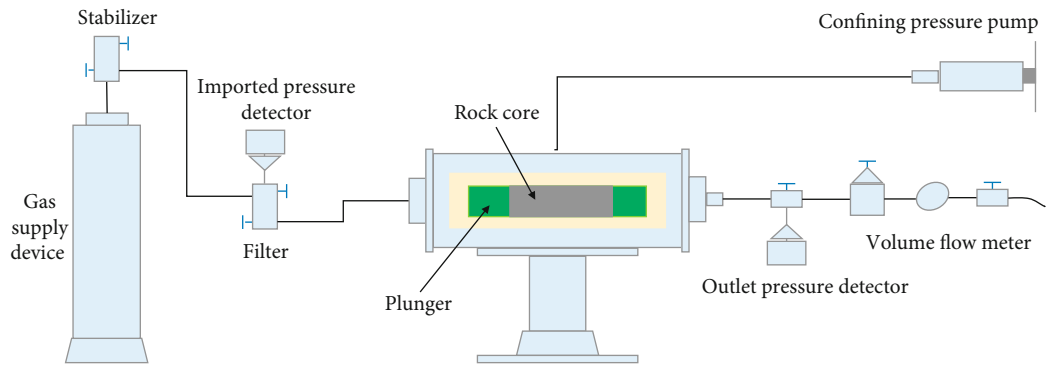

Figure 2: Experimental flowchart.

water can be recycled as water for fire-fighting in mining areas and sanitary water for office buildings. The treated concentrated brine is pumped to the underground storage for storage.

2.2. Research Methodology

2.2.1. Data Collection. Porosity and permeability are the two most important parameters of underground storage. In this study, actual samples of the underground concentrated brine storage reservoir floor were taken, and 3 samples were drilled using a core drilling device for permeability experiments. The experimental flowchart is shown in Figure 2, and the experimental results are shown in Table 1.

In order to ensure the accuracy of the experimental results and reduce the influence of experimental errors on the results, this study conducted three tests on each core by changing the inlet pressure and constructed the relationship curve between permeability and the pressure reciprocal. If the permeability has a linear relationship with the pressure

Table 1: Permeability test results.

Core name	No.	Length (mm)	Diameter (mm)	Porosity (%)	Inlet pressure (MPa)	Pressure reciprocal (1/MPa)	Permeability (mD)	Klinkenberg permeability (mD)
Underground storage floor	1	43.24	25.29	8.01	0.2139	4.6752	0.0592	0.0328
					0.3488	2.867	0.0495	
					0.4788	2.0884	0.0444	
	2	37.26	25.22	4.95	0.1918	5.2143	0.148	0.098
					0.2866	3.4892	0.1349	
					0.5432	1.8411	0.1147	
	3	41.04	24.49	4.12	0.3056	3.2719	0.0257	0.0106
					0.4426	2.2596	0.02	
					0.5608	1.7831	0.0193	

reciprocal, it indicates that the experimental results are accurate. The relationship between permeability and pressure reciprocal is shown in Figure 3.

The linear relationship between permeability and pressure reciprocal shows that the experimental results are accurate. According to the experimental results, the permeability coefficient of the underground storage floor is between 0.01 and 0.09 mD, which belongs to the ultralow permeability type. The results of this experiment provide basic data for the follow-up study to establish a physical model of the mining area. The calculation parameters are selected as shown in Table 2.

2.2.2. Physical Model. In this study, the salinity of concentrated brine was selected as the characteristic pollution factor. When the simulated value of the salinity exceeds the background concentration, it is considered that pollution has occurred. The model simulated the changes of diffusion distance, contaminated area, and salinity at the outer wall of the underground storage when the concentrated brine was sealed for 30 years, 50 years, and 70 years and sudden leakage for 30 days, 60 days, and 90 days, respectively. In this way, the influence of different time and different permeability coefficients on the migration of concentrated brine can be judged. Based on the actual hydrogeological conditions of Ling Xin Coal Mine, a constant groundwater head was set around the location of the underground storage on the model. Under the premise of keeping the model's horizontal and vertical groundwater head pressure differences the same, the head pressure differences are set to 10 meters, 50 meters, and 100 meters to simulate the influence of groundwater pressure field changes on the migration of concentrated brine.

The underground concentrated brine storage reservoir in the model is about 1,000 meters long from north to south, 1,500 meters wide from east to west, and about 95 meters high vertically. It is located in the 14th, 15th, and 16th coal seam goaf area, with a high west and low east, and a dip angle of about 10°. The water barrier at the bottom of the 16th coal separates the underground storage from the Bao Ta Mountain confined aquifer, which is all 7.6 meters thick and has a very low permeability coefficient.

The model is divided into 9216 square grids with a side length of 125 meters and a total simulation range of 196.16 km^2. In addition, the model is divided into 9 layers vertically, including the 14th, 15th, and 16th coal seams, 1 aquifer, 3 weak aquifers, 1 confined aquifer, and 1 weak aquifer (Figure 4). Under the sudden leak simulation scenario, the permeability coefficient of the bottom water barrier changes from 7*E*-11 to 1*E*-6, which is divided into two parts with an area of about 50,000 m^2.

In addition, in order to effectively observe the groundwater level changes around the mining area and facilitate the identification and verification of the model, head observation wells are set in the model. The location distribution of the observation wells is shown in Figure 1, and the geographic location is shown in Table 3.

2.2.3. Mathematical Model. This study established a concentrated brine flow-solute transport coupling model, in which the mathematical model is composed of groundwater flow differential equations and pollutant transport differential equations. Based on the groundwater flow differential equations and the geological characteristics of the storage, a three-dimensional unsteady groundwater transport equation and model boundary conditions were constructed. Then, the finite element method is used for numerical solution. Equations (1)–(5) are as follows:

$$\frac{\partial}{\partial x}\left(K_x\frac{\partial H}{\partial x}\right)+\frac{\partial}{\partial y}\left(K_y\frac{\partial H}{\partial y}\right)+\frac{\partial}{\partial z}\left(K_z\frac{\partial H}{\partial z}\right)+W=S\frac{\partial H}{\partial t}(x,y,z)\in D, \tag{1}$$

$$K_x\left(\frac{\partial H}{\partial x}\right)^2+K_y\left(\frac{\partial H}{\partial y}\right)^2+K_z\left(\frac{\partial H}{\partial z}\right)^2-\frac{\partial H}{\partial z}(K_z+p)+p=\mu\frac{\partial H}{\partial t}(x,y,z)\in \Gamma_o, \tag{2}$$

$$H(x,y,z)|_{t=0}=H_1(x,y,z)(x,y,z)\in D, \tag{3}$$

$$H(x,y,z,t)|\Gamma_1=H_1(x,y,z,t)(x,y,z)\in \Gamma_1, t>0, \tag{4}$$

$$K_n\frac{\partial H}{\partial n}\Big|\Gamma_2=q(x,y,z,t)(x,y,z)\in \Gamma_2, t>0. \tag{5}$$

D is the seepage area; H is the groundwater level, m; K_x, K_y, K_z are the permeability coefficients along the x, y,

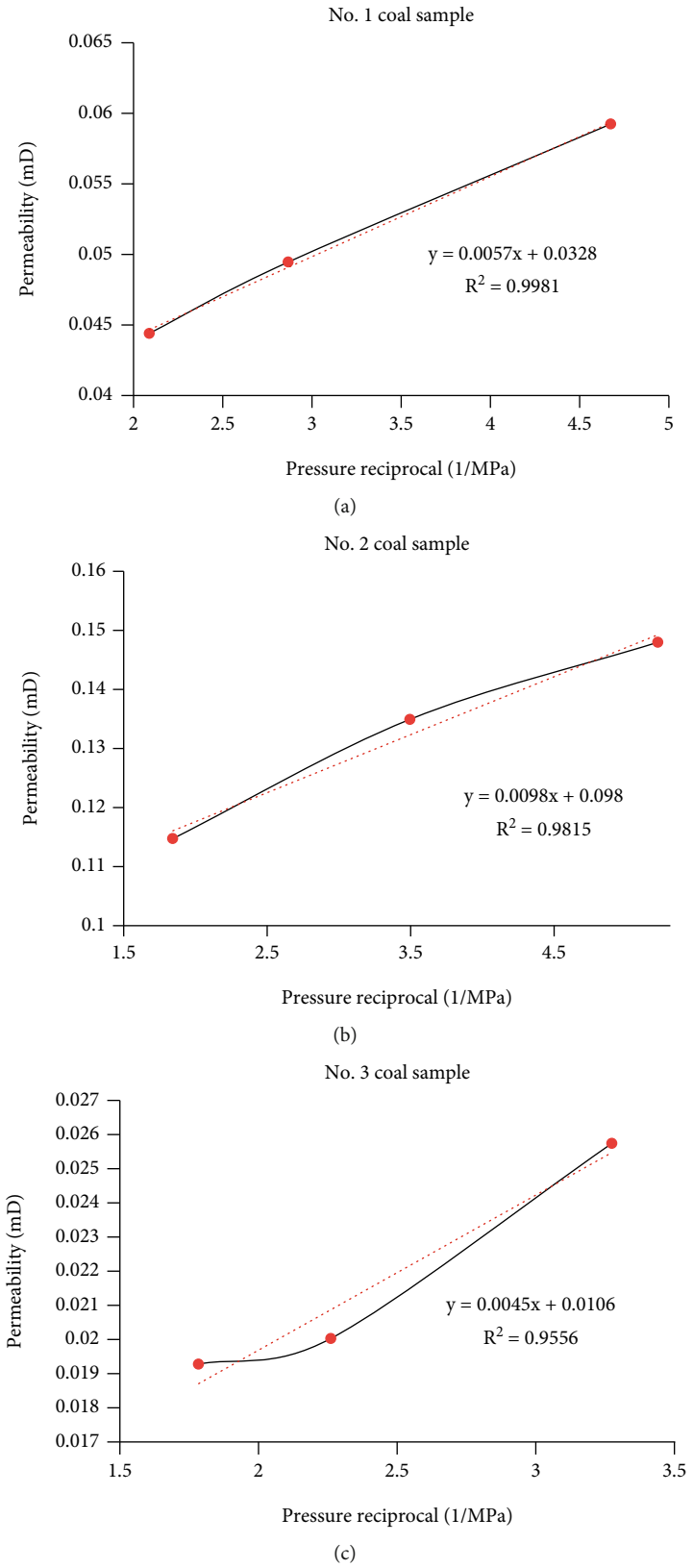

Figure 3: Relationship between permeability and pressure reciprocal.

Table 2: Selection of calculation parameters.

Parameter	Unit	Numerical value
Water barrier permeability coefficient under natural conditions	m/s	7*E*-11
Water barrier permeability coefficient under sudden leak	m/s	1*E*-6
Coal seam permeability coefficient	m/s	5*E*-8
Weak barrier-1 permeability coefficient	m/s	3*E*-9
Weak barrier-2 permeability coefficient	m/s	2*E*-9
Fluid density	kg/m^3	1000
Hydrodynamic viscosity	Pa·s	0.001
Fluid diffusion coefficient	m^2/d	1*E*-9
Concentrated brine salinity	mg/L	36000
Longitudinal dispersion coefficient	m	10
Horizontal to longitudinal dispersion ratio	1	0.1
Vertical to longitudinal dispersion ratio	1	0.01
Water storage rate	1/m	1*E*-5
Gravity water supply	1	0.2
Effective porosity	1	0.15
Total porosity	1	0.3

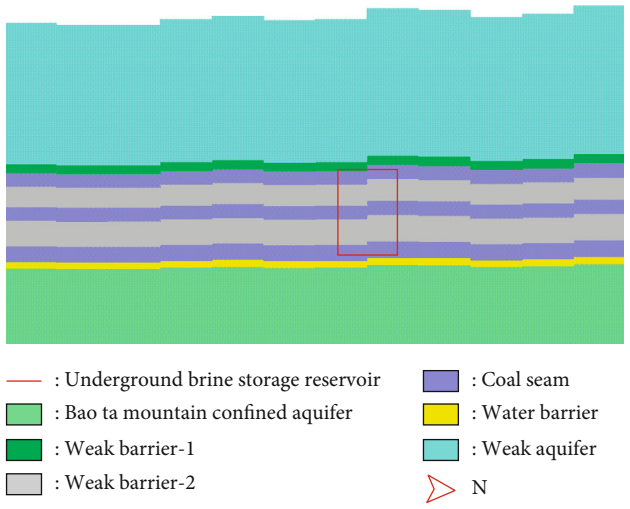

Figure 4: Vertical schematic diagram of underground concentrated brine storage reservoir (the model is stretched 20 times the actual vertical direction) (the model is stretched 20 times the actual vertical direction).

Table 3: Geographical location of observation wells.

Observation well	Latitude	Longitude
WELL-A	38° 04′ 40.5″	106° 38′ 47.5″
WELL-B	38° 02′ 15.4″	106° 39′ 8.4″
WELL-C	38° 05′ 19.20″	106° 39′ 42.79″
WELL-D	38° 05′ 19.14″	106° 38′ 21.24″

and z coordinate axes, m/d; S is the water storage coefficient, $1/m$; W is the sources and sinks of confined aquifers, $1/d$; p is the groundwater recharge, $1/d$; $H_0(x, y, z)$ is the initial head of flow field, m; $H_1(x, y, z)$ is the first-class boundary head, m; $q(x, y, z)$ is the single-width traffic on the second-class boundary, m^2/d; Γ_1 is the first boundary of seepage area; Γ_2 is the second boundary of seepage area; K_n is the permeability coefficient, m/d.

Pollutant transport differential Equations (6)–(11) are as follows:

$$\Delta M = -\left[\frac{\partial}{\partial x}(nF_x) + \frac{\partial}{\partial y}(nF_y) + \frac{\partial}{\partial z}(nF_z)\right]\Delta x\Delta y\Delta z\Delta t, \quad (6)$$

$$\Delta N = -\left[\frac{\partial}{\partial x}(nu_xC) + \frac{\partial}{\partial y}(nu_yC) + \frac{\partial}{\partial z}(nu_zC)\right]\Delta x\Delta y\Delta z\Delta t, \quad (7)$$

$$\Delta M_I = I\Delta x\Delta y\Delta z\Delta t, \quad (8)$$

$$\begin{aligned}\Delta M' &= (nC\Delta x\Delta y\Delta z)|_{t+\Delta t} - (nC\Delta x\Delta y\Delta z)|_t \\ &= \frac{\partial}{\partial t}(nC\Delta x\Delta y\Delta z)\Delta t,\end{aligned} \quad (9)$$

$$\Delta M' = \Delta M + \Delta N + \Delta M_I, \quad (10)$$

$$\frac{\partial nC}{\partial t} = \frac{\partial}{\partial x_i}\left(nD_{ij}\frac{\partial C}{\partial x_j}\right) - \frac{\partial nu_iC}{\partial x_i} + I, (i, j = x, y, z). \quad (11)$$

ΔM is the hydrodynamic dispersion increases the total mass of pollutants in the unit; ΔN is the convection increases the total mass of pollutants in the unit; ΔM_I is the source-sink effect increases the total mass of pollutants in the unit; $\Delta M'$ is the change in the quality of pollutants in the unit; $\Delta x, \Delta y, \Delta z$ is the side length of infinitely small hexahedron in space; u_x, u_y, u_z is the actual groundwater velocity in the direction of the coordinate axis; F_x, F_y, F_z is the pollutant dispersion flux in the direction of the coordinate axis; C is the pollutant concentration; Δt is the time interval; I is the

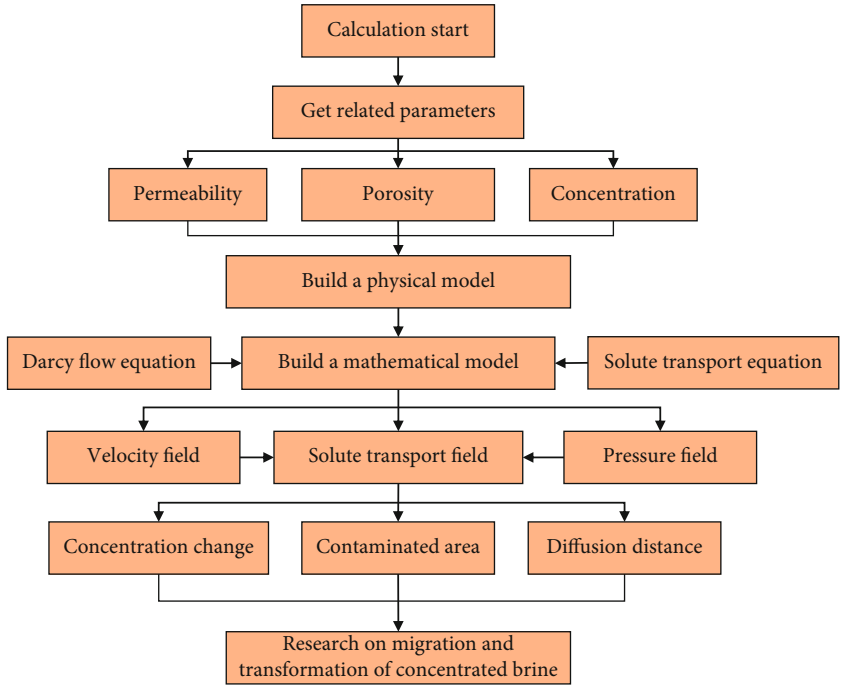

Figure 5: Block diagram of the calculation process.

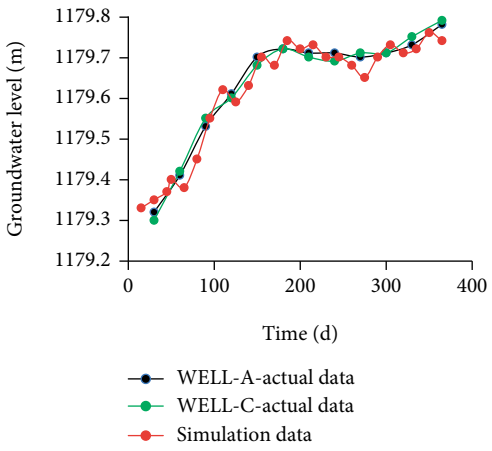

Figure 6: Model verification results.

Table 4: Test error statistics.

Observation well	R_e	R^2
WELL-A	0.19	0.774
WELL-C	0.17	0.783

porous media per unit time and unit volume get pollutant mass.

2.2.4. Model Identification and Verification. The correlation error method and relative coefficient method are used to identify and verify the model. Relevant calculation Equations (12) and (13) are as follows:

Relative error (R_e):

$$R_e = \frac{1}{n}\sum_{t=1}^{n}\left(\frac{|P_{st} - P_{obt}|}{\max_{(P_{obt})} - \min_{(P_{obt})}}\right) \times 100\%. \quad (12)$$

Correlation coefficients (R^2):

$$R^2 = \frac{\left[\sum_{t=1}^{n}\left(P_{obt} - \bar{P}_{ob}\right)\left(P_{st} - \bar{P}_s\right)\right]^2}{\sum_{t=1}^{n}\left(P_{obt} - \bar{P}_{ob}\right)^2\left(P_{st} - \bar{P}_s\right)^2}. \quad (13)$$

P_{obt} is the observed value of groundwater level in time t, m; P_{st} is the simulated value of groundwater level in time t, m; $\bar{P}_{ob}$ is the average measured groundwater level, m; $\bar{P}_s$ is the average simulated groundwater level, m; $\max_{(P_{obt})}$ is the maximum observed value of groundwater level, m; $\min_{(P_{obt})}$ is the minimum observation value of groundwater level, m.

2.2.5. Calculation Process. First, according to the hydrogeological conditions of the mining area, a physical model of underground concentrated brine storage reservoir is established on the basis of obtaining relevant parameters, such as permeability, porosity, and concentration. Then, based on the Darcy flow equation and the solute transport equation, a concentrated brine flow-solute transport coupling model is constructed on this basis. Then, the pollutant velocity field and pressure field are calculated by the model, and then, the pollutant transport field is obtained. From the solute transport simulation results, the changes in the diffusion distance and the contaminated area of concentrated brine as well as the changes in the salinity of underground reservoir outer wall can be analyzed. Finally, the migration law of

Table 5: Part of the simulation data under different groundwater head differences during 30 years of long-term penetration.

Groundwater head difference	Diffusion distance/m			Polluted area/m^2	Salinity/mg/L		
	North side	West side	Downside	North side	North side	West side	Downside
10 m	16.1	0.1	1.1	2967.43	10415	5645	8315
50 m	97.3	1.3	0.6	46399.09	15115	6015	6915
100 m	143	1.7	0.5	80284.28	20115	6115	6815

concentrated brine in the underground concentrated brine storage reservoir is summarized according to the simulation data. The block diagram of the calculation process is shown in Figure 5.

3. Results and Discussion

3.1. Model Identification and Verification. Before the formal simulation, the calculation parameters need to be modified and adjusted repeatedly under the premise that they are true. The model needs to reach a certain accuracy so that the simulated situation can be well fitted to the actual situation.

In this study, the groundwater level data of the Ling Xin mining area from 2018 to 2019 was first identified. Then, select the above-mentioned measured data to fit the simulation data of the head observation wells WELL-A and WELL-C. The model verification results are shown in Figure 6.

The numerical simulation result is compared with the measured value, and the relative error and correlation coefficient between the simulated value and the measured data are calculated to verify the simulation accuracy of the model. The model test error statistics are shown in Table 4.

It can be seen from Figure 6 that the data fit is better. However, this study only selected 365 days of measured data to fit the simulated data, and there is still a gap between the accuracy of the model and the reality. According to the statistical results of test errors in Table 4, the relative errors of the two observation wells are 0.19 and 0.17, respectively, and the error values are both small. And the correlation coefficients of the two observation wells are 0.774 and 0.783, respectively, which are both greater than 0.5. The above shows that the model can reflect the actual change trend of the groundwater level in the study area.

3.2. Migration of Concentrated Brine in Underground Storage under Long-Term Penetration Scenarios. By setting the model conditions, the long-term penetration simulation scenarios are divided into 30 years, 50 years, and 70 years.

3.2.1. Long-Term Penetration for 30 Years. When the long-term penetration period is 30 years, some simulation data and model diagrams under different groundwater head differences are shown in Table 5 and Figure 7. From the value of diffusion distance, polluted area, and salinity, it can be found that with the increase of groundwater head difference, the migration of concentrated brine to the north and west side of underground storage also deepens, and the migration to the north side increases more significantly. On the contrary, the downward migration of the concentrated brine decreases with the increase of the groundwater head difference. The reason for this phenomenon may be that the increase of the groundwater head difference causes the speed of the groundwater outside the underground storage to increase, and the movement of the concentrated brine in the underground storage is affected. When the groundwater head difference is small, the penetration pressure formed by the concentrated brine under its own gravity on the bottom water barrier is greater, and it is easier to penetrate it.

It can be clearly seen from Figure 7 that the water barrier layer has a great water barrier effect, and the maximum diffusion distance is only about 1 meter. However, the permeability coefficient of the rock formation on the north side of the underground storage is larger, so the permeability distance is farther. In general, after 30 years of long-term penetration, the migration of concentrated brine is relatively weak, and there is no adverse effect on the surrounding environment of the underground storage.

Under the 30 years of simulation scenario of long-term infiltration, the relationship between the diffusion distance of concentrated brine and the change in groundwater head difference and the relationship between the mineralization of the outer wall of the storage and the change in groundwater head difference are shown in Figure 8. Within a certain range of groundwater head difference, there is a linear correlation between the diffusion distance of concentrated brine and the change of groundwater head difference. The increase of the groundwater head difference means the increase of the groundwater pressure difference and the acceleration of the groundwater flow rate outside the underground storage. The movement of concentrated brine in underground storage is also affected by the velocity and flow of groundwater outside the storage. Similarly, within a limited range of head pressure difference, the concentration of brine salinity at the outer wall of the underground storage has a linear relationship with the groundwater head difference. The greater the difference in ground-water head, the higher the degree of salinity of the concentrated brine on the outer wall of the underground storage, and the stronger the migration speed and migration capacity of the concentrated brine.

3.2.2. Long-Term Penetration for 50 Years. Compared with 30 years of long-term penetration, the added value of simulation data at 50 years is shown in Table 6, and part of the model diagram is shown in Figure 9. After the data is sorted, it can be clearly seen that the penetration pattern of concentrated brine with the groundwater head difference after 50 years of long-term penetration is basically the same as the penetration pattern of concentrated brine after 30 years of

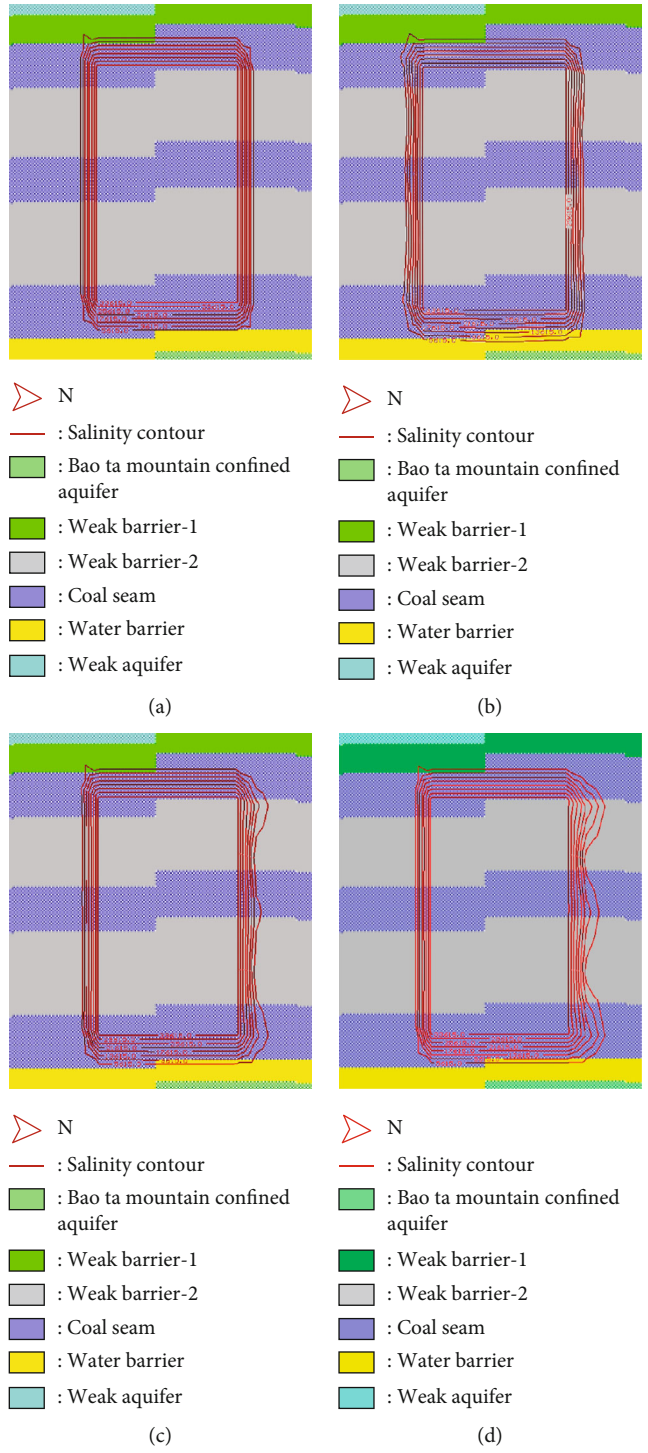

Figure 7: The migration of concentrated brine to the north side under different groundwater head differences after long-term penetration for 30 years (the model is stretched 20 times the actual vertical direction, (a) is the initial state, (b) is 10 meters, (c) is 50 meters, and (d) is 100 meters).

long-term penetration. Among them, the downward permeability changes of concentrated brine are still opposite to those on the north and west sides, and this rule is more obvious when compared with the 30 years of simulation scenario of long-term penetration. In addition, it can be seen from the comparative analysis of the long-term sequence that under the same groundwater head difference condition, as the storage time of the concentrated brine increases, the migration slowly deepens. Especially when the groundwater head difference is 100 meters, the increase in the polluted area and diffusion distance of the concentrated brine to the north is the most significant. In summary, the migration of

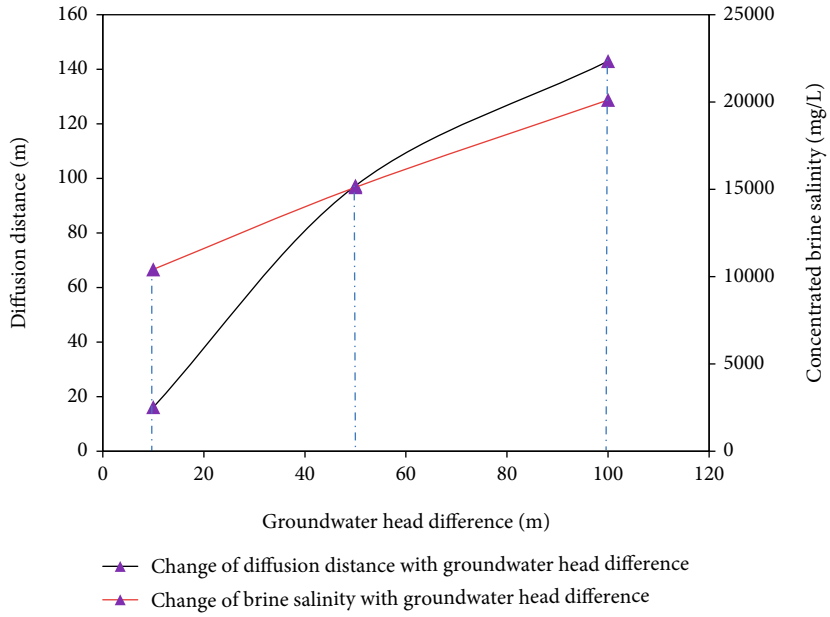

Figure 8: Relationship curve between the diffusion distance of concentrated brine, the groundwater head difference, and the salinity at the outer wall of the underground storage after 30 years of long-term penetration.

Table 6: Increase in simulated data for 50 years of long-term penetration compared to 30 years of long-term penetration.

Groundwater head difference	Diffusion distance/m			Polluted area/m^2	Salinity/mg/L		
	North side	West side	Downside	North side	North side	West side	Downside
10 m	31.1	0.1	0.7	8048.25	1200	50	1570
50 m	39.3	0.9	0.1	33228.64	4000	235	480
100 m	115.4	2.9	0.1	57150.96	4750	770	285

concentrated brine to the north side is more susceptible to groundwater head difference and storage time than migration to the west side of the storage.

It can be seen from Figure 9 that it is difficult for the concentrated brine to penetrate into the bottom water barrier in its natural state. Even when the groundwater head difference is 10 meters, the concentrated brine only penetrates down 0.7 meters in 20 years. The bottom water barrier effectively avoids the adverse effects of the penetration of concentrated brine on the Bao Ta Mountain confined aquifer.

Under the 50 years of simulation scenario of long-term penetration, the relationship between the diffusion distance of concentrated brine and the change in groundwater head difference and the relationship between the salinity of the outer wall of the storage and the change in groundwater head difference are shown in Figure 10. The trend of the two curves is basically the same as that of the 30 years simulation scenario, but there are still differences. Although the salinity of concentrated brine on the outer wall of underground storage still increases with the increase in groundwater head difference, the increase slows down. With the increase of the groundwater head difference and the prolongation of the extravasation time of the concentrated brine, the penetration amount of the concentrated brine to the north side increased. In addition, as the salinity of the concentrated brine in the storage gradually decreases, the difference in salinity between the inside and outside of the underground storage is reduced, and the driving force for the penetration of the concentrated brine in the storage is also weakened.

3.2.3. Long-Term Penetration for 70 Years. In the case of different groundwater head differences, the simulation data changes of 70 years of long-term penetration compared with 50 years are shown in Table 7, and the model diagram of long-term penetration of 70 years is shown in Figure 11. As a result, it can be found that at a groundwater head difference of 10 meters, the concentrated brine finally penetrated the bottom water barrier into the Bao Ta Mountain confined aquifer at 62 years after a long period of penetration. What is more, it can be clearly seen from the increase in salinity of the concentrated brine at the lower side of 4510 mg/L when the groundwater head difference is 10 meters that the penetration rate of the concentrated brine after entering the Bao Ta Mountain confined aquifer is significantly faster and the migration capacity is rapidly enhanced. Due to the reasons analyzed above, the underground storage reservoir and the surrounding groundwater environment as a whole are at a higher risk.

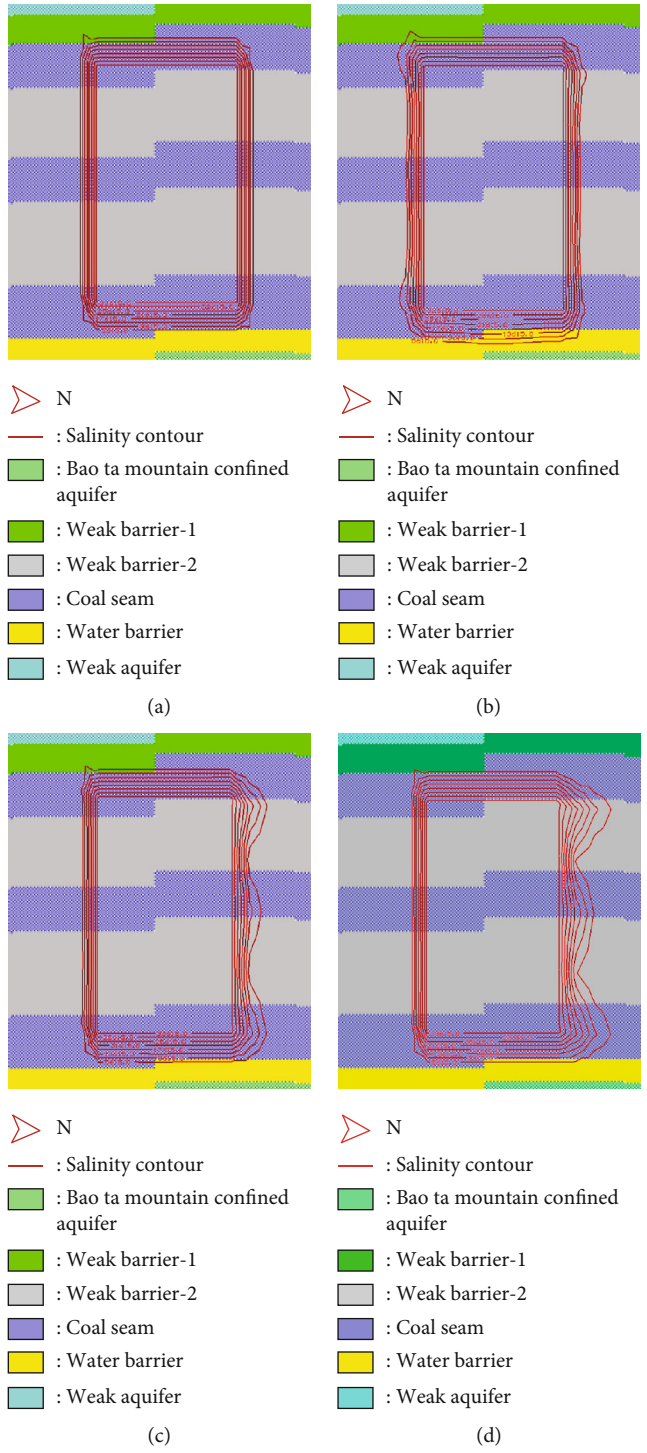

Figure 9: The migration of concentrated brine to the north side under different groundwater head differences after long-term penetration for 50 years (the model is stretched 20 times the actual vertical direction, (a) is the initial state, (b) is 10 meters, (c) is 50 meters, and (d) is 100 meters).

Under the 70 years of simulation scenario of long-term penetration, the relationship between the diffusion distance of concentrated brine and the salinity of the outer wall of underground storage and the groundwater head difference is shown in Figure 12. As the groundwater head difference increases, compared with the 50 years simulation scenario of long-term penetration, the rising trend of the salinity of the outer wall of the underground storage has slowed down more obviously. At the same time, the migration distance of concentrated brine also shows a slowing down trend. In the case of a higher groundwater head difference, the longer the time of continuous extravasation of the concentrated brine, the larger the diffusion distance and the polluted area. However, the increase has changed from high to low.

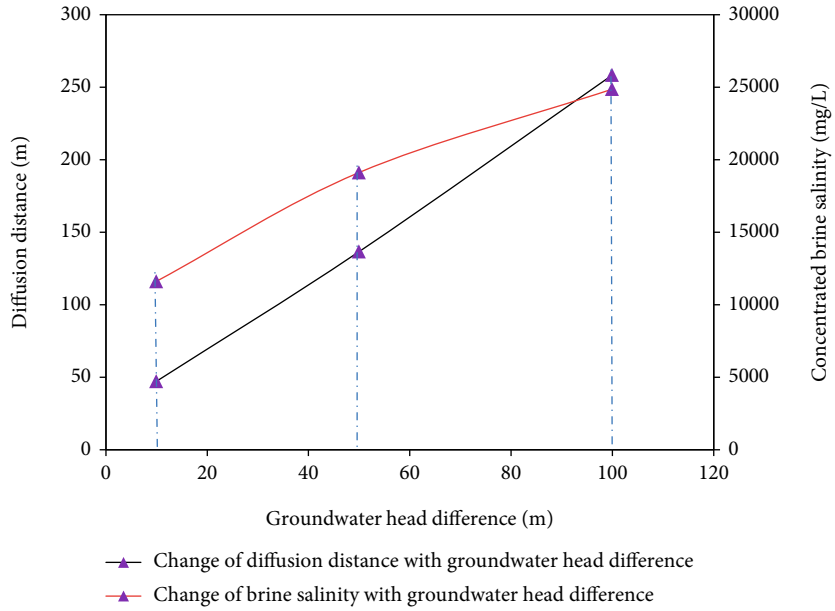

Figure 10: Relationship curve between the diffusion distance of concentrated brine, the ground-water head difference, and the salinity at the outer wall of the underground storage after 50 years of long-term penetration.

Table 7: Increase in simulated data for 70 years of long-term penetration compared to 50 years of long-term penetration.

Groundwater head difference	Diffusion distance/m			Polluted area/m^2	Salinity/mg/L		
	North side	West side	Downside	North side	North side	West side	Downside
10 m	28.9	0.1	9.6	14495.73	1150	10	4510
50 m	70.3	0.9	0.1	29218.03	3000	245	270
100 m	55.2	1.8	0.1	39161.51	2250	500	335

Through the long-term penetration simulation scenario, it can be known that the migration patterns of concentrated brine are as follows. The migration of concentrated brine in underground storage during long-term penetration is mainly affected by storage time and groundwater head difference. The storage time mainly affects the degree of migration of the concentrated brine. With the extension of storage time, the migration of concentrated brine increases slowly, mainly to the north side of the storage. The groundwater head difference mainly affects the movement state of the concentrated brine in the underground storage. When the groundwater head difference is small, the concentrated brine mainly migrates downward, and when the groundwater head difference gradually increases, the main migration direction of the concentrated brine turns to the north side of the reservoir. This is related to the direction of groundwater flow in the mining area. When the groundwater head difference is large, the extravasation volume of the concentrated brine gradually increases with the continuous extension of the outward penetration time, and the polluted area, diffusion distance, and salinity of the outer wall of the storage also increase. But at the same time, the salinity of the concentrated brine in the storage is reduced, the difference in salinity between the inside and outside of the storage is reduced, and the dynamics of the extravasation of the concentrated brine is attenuated. This reduces the extravasation rate of concentrated brine. Through long-term penetration simulation, an emergency plan is provided for the management and control of the long-term penetration risk of concentrated brine under actual conditions.

3.3. Migration of Concentrated Brine in Underground Storage under Sudden Leak Scenarios. Since there are still coal seams near the underground storage that continue to be mined, there is a possibility that the permeability of the bottom water barrier may change due to the disturbance of man-made coal mining or other natural reasons. In the case of a sudden increase in the permeability coefficient of the bottom water barrier, the large-scale leak of the concentrated brine may further aggravate the migration of the concentrated brine. Therefore, in order to explore the migration trend of concentrated brine during emergencies, the partial permeability coefficient of the water barrier in the model was increased from 7*E*-11 in the natural state to 1*E*-6 when the emergency occurred. At the same time, combined with the long-term natural penetration simulation results, the groundwater head pressure difference is set to 10 meters, and the simulation time is set to 30 days, 60 days, and 90 days. See Table 8 for simulation data.

Figure 13 shows the migration of concentrated brine to the water barrier at different times under the sudden leak scenario. When the sudden leak occurred for 30 days, the

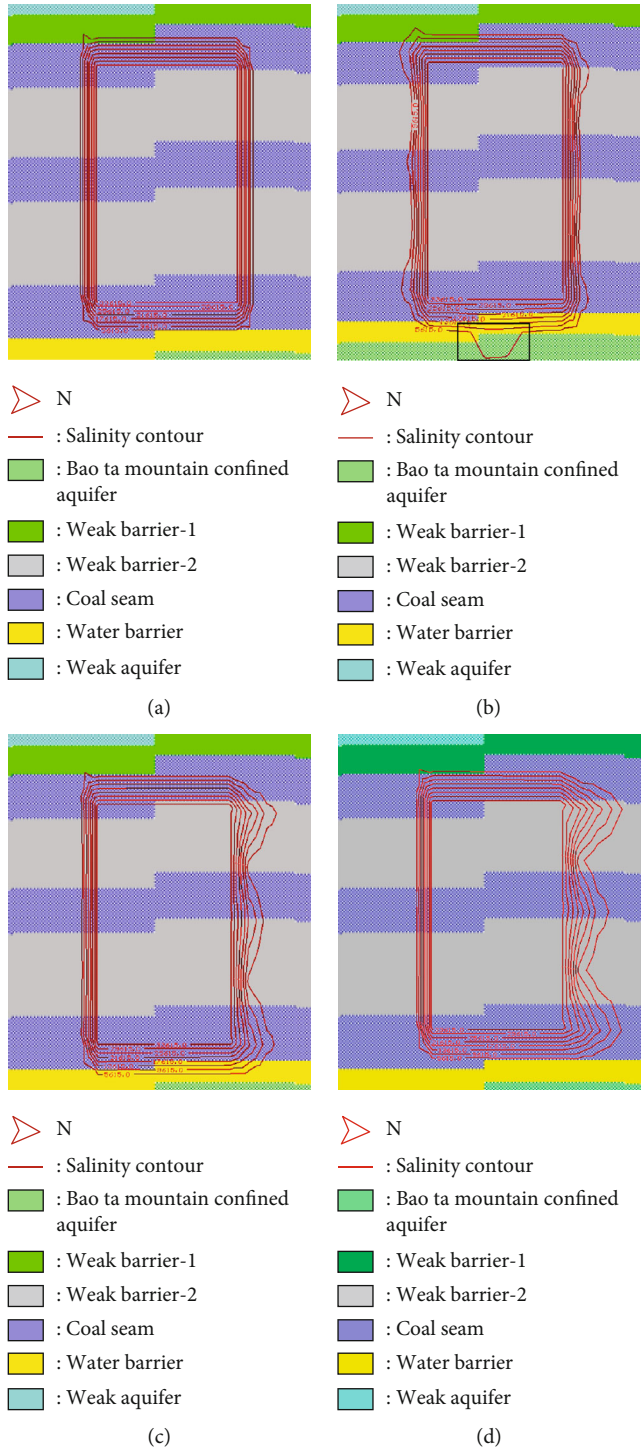

Figure 11: The migration of concentrated brine to the north side under different groundwater head differences after long-term penetration for 70 years (the model is stretched 20 times the actual vertical direction, (a) is the initial state, (b) is 10 meters, (c) is 50 meters, and (d) is 100 meters).

concentrated brine penetrated 1.0 m into the aquifer, with a polluted area of 97425.7 m^2, and the salinity of the water barrier was 8295 mg/L. Within 30 days, the downward penetration rate of concentrated brine accelerated, but it still did not penetrate the bottom water barrier. It can be seen that when an emergency occurs, the downward migration of concentrated brine is within a safe range within 30 days. However, when there was a sudden leak for 38 days, the concentrated brine penetrated the bottom water barrier downward. At 60 days, the brine penetrated up to 23.7 meters to the lower side, an increase of 22.7 meters compared with 30 days. At the same time, the polluted area is 209145.29 m^2, which is an increase of 111719.59 m^2, and the salinity of the water barrier is 11115 mg/L, which is an

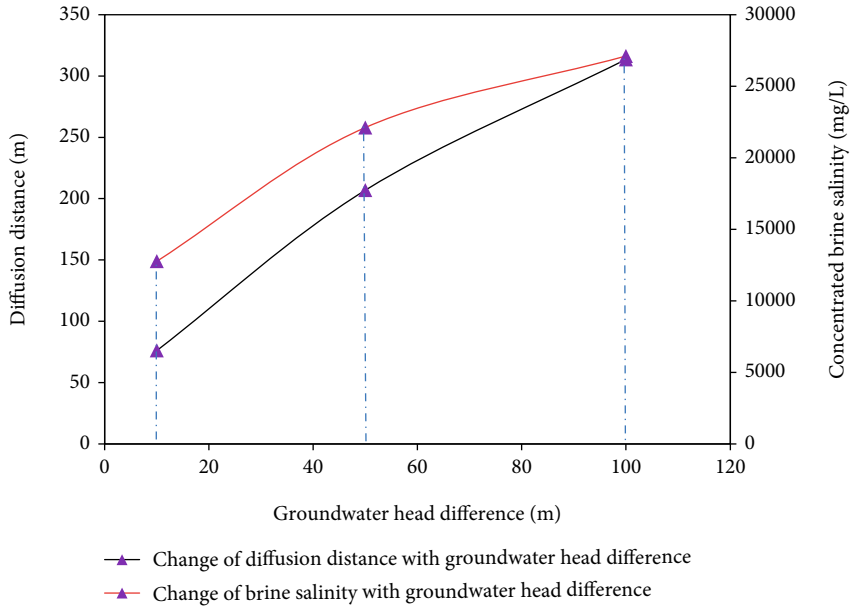

Figure 12: Relationship curve between the diffusion distance of concentrated brine, the ground-water head difference, and the salinity at the outer wall of the underground storage after 70 years of long-term penetration.

Table 8: Partial simulation data of different sudden leak times when the groundwater head difference is 10 meters.

Sudden leak time	Diffusion distance/m	Polluted area/m^2	Salinity change/ mg/L
30 d	1.0	97425.7	8295
60 d	23.7	209145.29	16115
90 d	34.5	244230.21	19695

increase of 7820 mg/L. It can be seen that before the concentrated brine penetrates the water barrier, the migration speed is slow, and the movement is relatively stable. After the concentrated brine penetrates the water barrier and enters the aquifer, the migration speed increases sharply, and the movement speed increases significantly. After 90 days of sudden leak, the scope of influence was further expanded. However, from the comparison of the 30 days to 60 days data and the 60 days to 90 days data increase in Figure 14, it can be seen that the concentration of the concentrated brine in the underground concentrated brine storage reservoir decreases with the leak of the concentrated brine, the penetration power decreases, and the migration speed slows down. This is the same as the migration pattern of concentrated brine obtained under the long-term penetration simulation scenario.

Under the sudden leak simulation scenario, the influence of the reservoir permeability coefficient on the migration of concentrated brine to the bottom water barrier is mainly explored. After the permeability coefficient of the bottom water barrier increases suddenly, the downward migration speed of the concentrated brine is significantly accelerated, and it only takes 38 days to penetrate the water barrier. The migration speed and ability of the concentrated brine after entering the Bao Ta Mountain confined aquifer is enhanced on this basis, which is directly reflected in the expansion of the concentrated brine polluted area and the increase in the diffusion distance. With the extension of the sudden leak time, the migration speed and migration capacity of the concentrated brine in the underground storage are gradually decreasing, and the increase of various indicators decreases. This phenomenon is consistent with the results of previous studies. The results of the sudden leakage simulation are close to reality, and it is of great significance to accurately put forward 30 days as a key period to curb the spread of concentrated brine.

3.4. Analysis of Influencing Factors on Long-Term Penetration and Sudden Leak of Underground Concentrated Brine Storage Reservoir. In the long-term penetration simulation scenario, the diffusion distance of the concentrated brine to the north side of the storage under different groundwater head differences is shown in Figure 15. At the same simulation time, within a certain range of groundwater head difference, the northward diffusion distance of concentrated brine increases with the increase of groundwater head difference. And as the groundwater head difference increases, the increase in penetration distance changes from large to small. When the groundwater head difference remains the same, regardless of the value, the diffusion distance of the concentrated brine to the north side shows a gradual increase with the extension of the simulation time, but the increase rate changes from high to low. The migration of the concentrated brine over time is first strong and then weak. It can be seen that under the long-term penetration scenario, the groundwater head difference and the penetration time are important factors influencing the migration of concentrated brine.

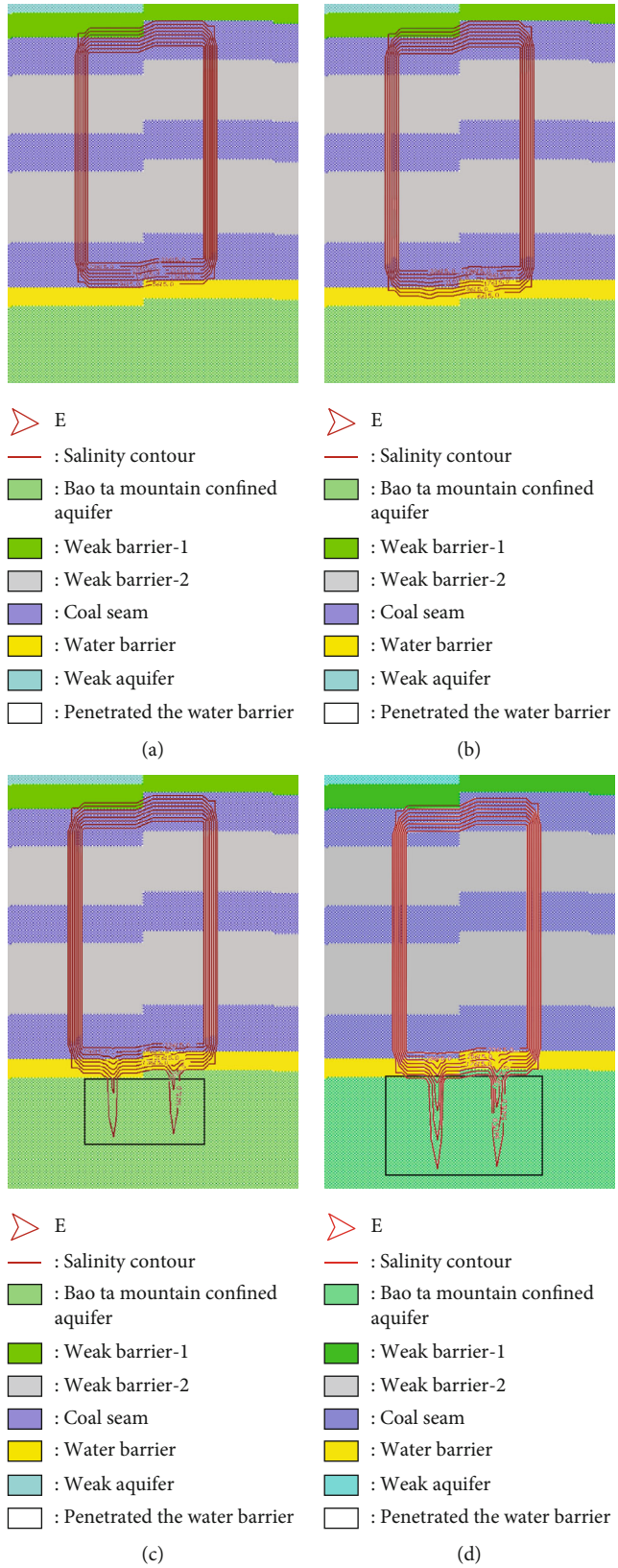

Figure 13: Migration of concentrated brine to the bottom water barrier at different times under sudden leak scenarios (the model is stretched 20 times the actual vertical direction, (a) is the initial state, (b) is 10 meters, (c) is 50 meters, and (d) is 100 meters).

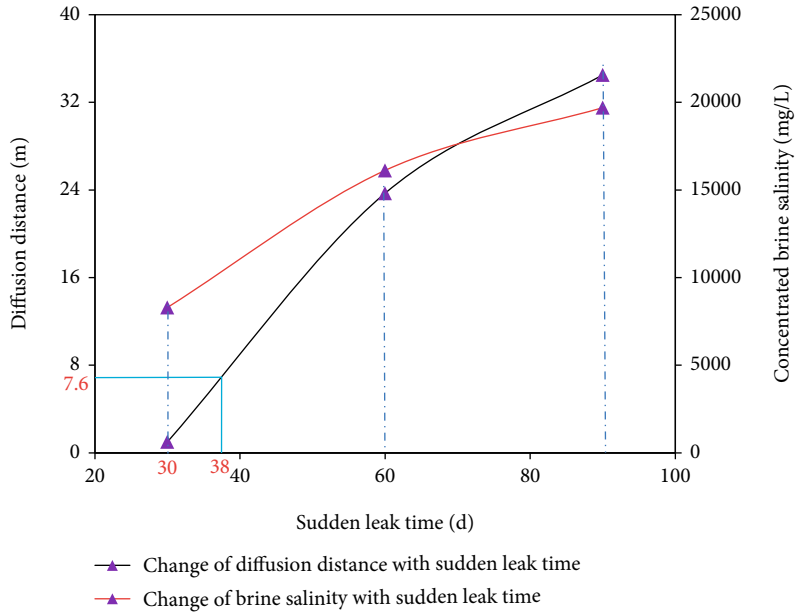

Figure 14: The relationship curve between the diffusion distance and salinity of concentrated brine and different sudden leak time.

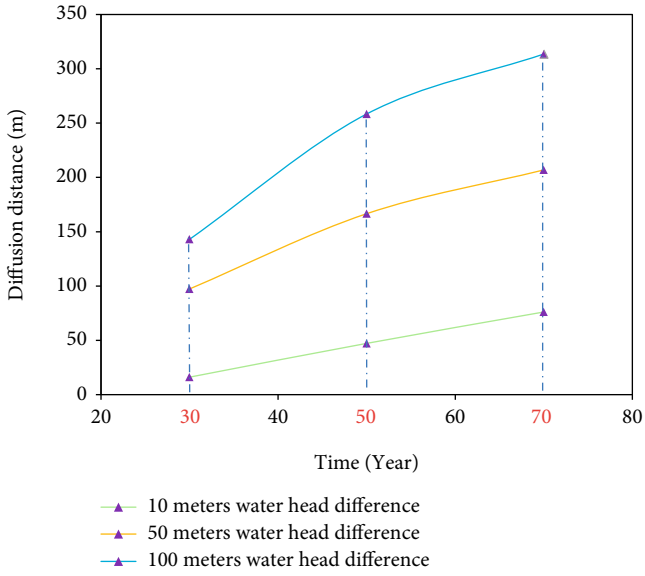

Figure 15: Comparison of the diffusion distance of concentrated brine to the north side at different groundwater head differences under long-term penetration scenarios.

From the long-term penetration and sudden leak simulation scenarios, the time-varying curve of the penetration distance of concentrated brine to the bottom water barrier can be known (Figure 16). After 38 days of sudden leak and 62 years of long-term penetration, the concentrated brine migrated more than 7.6 meters to the lower side of the storage and penetrated the water barrier. It can be clearly seen from the comparison of penetration time that when the permeability coefficient is extremely low, the migration of concentrated brine to the outside of the reservoir can be effectively inhibited. However, once the permeability coefficient increases, the movement of the concentrated brine in the underground storage will change significantly, and its migration will become more unstable. The permeability coefficient of underground concentrated brine storage reservoir is a key factor affecting the migration pattern of concentrated brine.

4. Conclusion

In this study, by consulting the hydrogeological data of the Ling Xin Coal Mine area, the parameters such as the permeability coefficient and porosity of the bottom water barrier were analyzed. Based on the finite difference commercial software, a coupled model of concentrated brine flow and solute transport in the underground concentrated brine storage reservoir of Ling Xin mining area was accurately established. The migration of concentrated brine in underground concentrated brine storage reservoir under different groundwater head differences, different permeability coefficients, and different storage time conditions is analyzed. In addition, this research provides reference and compliance for avoiding environmental risks in actual situations, and has practical and economic benefits.

When the long-term penetration was about 60 years and the sudden leak was about 40 days, the concentrated brine penetrated the water barrier and entered the Bao Ta Mountain confined aquifer. The migration ability of concentrated brine is obviously enhanced. In addition, the impact of sudden leakage under the two simulation scenarios is more serious, the migration speed and capacity of concentrated brine is stronger, the leakage is larger, the diffusion distance is longer, and the pollution area is wider. It is very important that the plan for the prevention and control of concentrated brine environmental pollution in the event of sudden leakage should be improved and supplemented.

Groundwater head difference, reservoir permeability coefficient, and storage time are important influencing

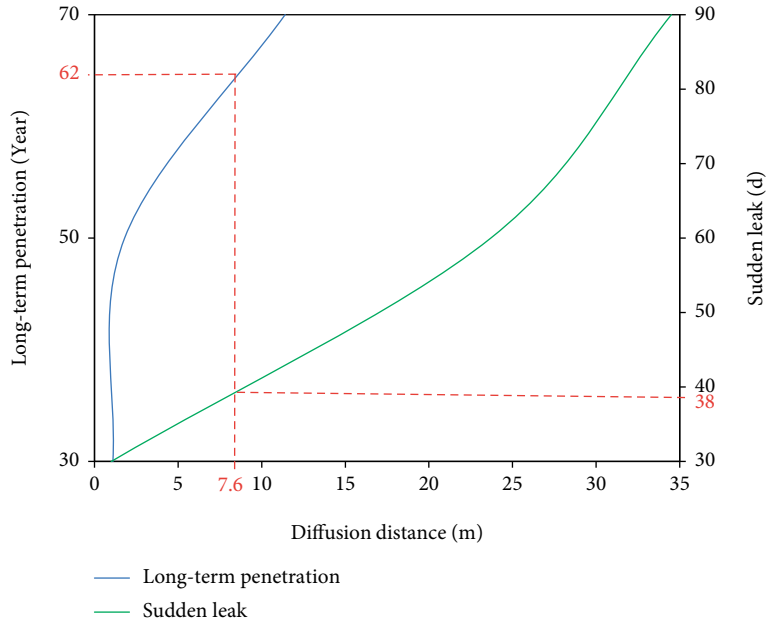

Figure 16: Curves of diffusion distance of concentrated brine to the water barrier with time for long-term infiltration and sudden leakage simulation scenarios.

factors affecting the migration of concentrated brine in underground storage reservoir, among which the reservoir permeability coefficient is the most critical. Strengthening the anticorrosion and antiseepage measures of the dam body and coal pillar during the construction of the underground concentrated brine storage reservoir can effectively prevent the occurrence of risks. In the case of sudden leakage, the permeability coefficient of the reservoir increases, the migration capacity of the concentrated brine increases sharply, and the time it takes to penetrate the water barrier is greatly shortened. In addition, the movement of concentrated brine in underground storage is significantly affected by the groundwater head difference outside the reservoir. During the same storage period, if the groundwater head difference is too high or too low, the migration of concentrated brine will increase accordingly.

Data Availability

Data is available on request. Please contact the corresponding author for the underlying data supporting the results of the research.

Conflicts of Interest

The authors declare no conflict of interest.

Authors' Contributions

X.H. and Z.D. are responsible for conceptualization and methodology; X.L. is responsible for software and validation; H.H. is responsible for formal analysis and investigation; X. S. is responsible for resources and data curation; J.G. is responsible for writing—original draft preparation; S.W. is responsible for writing—review and editing and visualization; G.K. is responsible for supervision and project administration. All authors have read and agreed to the published version of the manuscript.

Acknowledgments

The authors are grateful for financial support from the National Energy Group Ningxia Coal Industry Company Lingxin Coal Industry Demonstration Project (Environmental Risk Research of Underground Brine Storage Reservoir in Mining Area) and Open Fund of Chinese State Key Laboratory of Water Resource Protection and Utilization in Coal Mining with grant number SHJT-16-30.3. The authors would also like to thank the reviewers and editors whose critical comments were very helpful in preparing this article.

References

[1] B. Lin and R. Zhu, "Energy efficiency of the mining sector in China, what are the main influence factors?," *Resources, Conservation and Recycling*, vol. 167, article 105321, 2021.

[2] J. Chen, S. Wen, and Y. Liu, "Research on the efficiency of the mining industry in China from the perspective of time and space," *Resources Policy*, vol. 75, article 102475, 2022.

[3] X. Wang, Y. Gao, X. Jiang, Q. Zhang, and W. Liu, "Analysis on the characteristics of water pollution caused by underground mining and research progress of treatment technology," *Advances in Civil Engineering*, vol. 2021, 14 pages, 2021.

[4] X. Tang, Y. Jin, B. C. McLellan, J. Wang, and S. Li, "China's coal consumption declining–impermanent or permanent?," *Resources, Conservation & Recycling*, vol. 129, pp. 307–313, 2018.

[5] X. Zhang, Y. Dong, J. Zhao, B. Gong, Z. Meng, and J. Lin, "Combined treatments of underground coal slurry: laboratory testing and field application," *Water*, vol. 13, no. 21, article 3047, 2021.

[6] S. Du, X. Su, and W. Zhang, "Effective storage rates analysis of groundwater reservoir with surplus local and transferred water used in Shijiazhuang City, China," *Water and Environment Journal*, vol. 27, no. 2, pp. 157–169, 2013.

[7] S. N. Ashraf, J. Rajapakse, L. A. Dawes, and G. J. Millar, "Electrocoagulation for the purification of highly concentrated brine produced from reverse osmosis desalination of coal seam gas associated water," *Process Engineering*, vol. 28, pp. 300–310, 2019.

[8] D. Z. Gu, "Theory framework and technological system of coal mine underground reservoir," *Journal of China Coal Science*, vol. 40, no. 2, pp. 239–246, 2015.

[9] Q. Guo, "Research on the deep treatment of high salinity mine water and the storage technology of concentrated brine," vol. 52, no. 12, pp. 16–19, 2020.

[10] B. Jabłońska, "Sorption of phenol on rock components occurring in mine drainage water sediments," *International Journal of Mineral Processing*, vol. 104-105, pp. 71–79, 2012.

[11] J. Tan, H. Song, H. Zhang, Q. Zhu, Y. Xing, and J. Zhang, "Numerical investigation on infiltration and runoff in unsaturated soils with unsteady rainfall intensity," *Water*, vol. 10, no. 7, p. 914, 2018.

[12] P. T. Mativenga and A. Marnewick, "Water quality in a mining and water-stressed region," *Journal of Cleaner Production*, vol. 171, pp. 446–456, 2018.

[13] J. Li, Y. Huang, W. Li, Y. Guo, S. Ouyang, and G. Cao, "Study on dynamic adsorption characteristics of broken coal gangue to heavy metal ions under leaching condition and its cleaner mechanism to mine water," *Journal of Cleaner Production*, vol. 329, article 129756, 2021.

[14] P. Li, H. Qian, and J. Wu, "Conjunctive use of groundwater and surface water to reduce soil salinization in the Yinchuan Plain, North-West China," *International Journal of Water Resources Development*, vol. 34, no. 3, pp. 337–353, 2018.

[15] W. M. Mayes, E. Gozzard, H. A. B. Potter, and A. P. Jarvis, "Quantifying the importance of diffuse minewater pollution in a historically heavily coal mined catchment," *Environmental Pollution*, vol. 151, no. 1, pp. 165–175, 2008.

[16] P. Wu, C. Tang, C. Liu, L. Zhu, T. Pei, and L. Feng, "Geochemical distribution and removal of As, Fe, Mn and Al in a surface water system affected by acid mine drainage at a coalfield in southwestern China," *Environmental Geology*, vol. 57, no. 7, pp. 1457–1467, 2009.

[17] X. Wei, F. A. Wolfe, and Y. Li, "Mine drainage and oil sand water," *Water Environment Research*, vol. 87, no. 10, pp. 1373–1391, 2015.

[18] J. Wang, H. Song, and Y. Wang, "Investigation on the microflow mechanism of enhanced oil recovery by low-salinity water flooding in carbonate reservoir," *Fuel*, vol. 266, no. C, p. 117156, 2020.

[19] S. Chetty, L. Pillay, and M. S. Humphries, "Gold mining's toxic legacy: pollutant transport and accumulation in the Klip River catchment, Johannesburg," *South African Journal of Science*, vol. 117, no. 7/8, pp. 1–11, 2021.

[20] D. W. Qiao, J. Yao, L. J. Song, and J. Y. Yang, "Migration of leather tannins and chromium in soils under the effect of simulated rain," *Chemosphere*, vol. 284, article 131413, 2021.

[21] A. González-Quirós and J. P. Fernández-Álvarez, "Conceptualization and finite element groundwater flow modeling of a flooded underground mine reservoir in the Asturian Coal Basin, Spain," *Journal of Hydrology*, vol. 578, no. C, p. 124036, 2019.

[22] Y. Sun, S. G. Xu, P. P. Kang, Y. Z. Fu, and T. X. Wang, "Impacts of artificial underground reservoir on groundwater environment in the reservoir and downstream area," *International Journal of Environmental Research and Public Health*, vol. 16, no. 11, p. 1921, 2019.

[23] X. Lin, J. Tang, Z. Li, and H. Li, "Finite element simulation of total nitrogen transport in riparian buffer in an agricultural watershed," *Sustainability*, vol. 8, no. 3, p. 288, 2016.

[24] D. Malinovsky, I. Rodushkin, T. Moiseenko, and B. Öhlander, "Aqueous transport and fate of pollutants in mining area: a case study of Khibiny apatite–nepheline mines, the Kola Peninsula, Russia," *Environmental Geology*, vol. 43, no. 1-2, pp. 172–187, 2002.

[25] N. Dalla Libera, D. Pedretti, G. Casiraghi, Á. Markó, L. Piccinini, and P. Fabbri, "Probability of non-exceedance of arsenic concentration in groundwater estimated using stochastic multicomponent reactive transport modeling," *Water*, vol. 13, no. 21, article 3086, 2021.

[26] K. Shamshad, S. Hatice, and D. Zhang, "Transport of TiO2 nanoparticles and their effects on the mobility of Cu in soil media," *Desalination and Water Treatment*, vol. 131, pp. 230–237, 2018.

[27] T. Miao and J. Guo, "Application of artificial intelligence deep learning in numerical simulation of seawater intrusion," *Environmental Science and Pollution Research*, vol. 28, no. 38, pp. 54096–54104, 2021.

[28] Z. Zhou, C. Wang, J. Bi, Y. Zhao, and W. Xiang, "Simulation of underground freshwater exploitation and analysis of environmental impact in Hangzhou Bay New Area, China," *Natural Resources Research*, vol. 30, no. 2, pp. 1781–1794, 2021.

[29] M. K. Singh, S. Rajput, and R. K. Singh, "Study of 2D contaminant transport with depth varying input source in a groundwater reservoir," *Water Supply*, vol. 21, no. 4, pp. 1464–1480, 2021.

[30] X. Guo, H. Song, J. Killough, L. Du, and P. Sun, "Numerical investigation of the efficiency of emission reduction and heat extraction in a sedimentary geothermal reservoir: a case study of the Daming geothermal field in China," *Environmental Science and Pollution Research International*, vol. 25, no. 5, pp. 4690–4706, 2018.

[31] T. Li, H. Song, J. Wang, Y. Wang, and J. Killough, "An analytical method for modeling and analysis gas-water relative permeability in nanoscale pores with interfacial effects," *International Journal of Coal Geology*, vol. 159, pp. 71–81, 2016.

[32] H. Fan, L. Zhang, R. Wang et al., "Investigation on geothermal water reservoir development and utilization with variable temperature regulation: a case study of China," *Applied Energy*, vol. 275, article 115370, 2020.

[33] H. Song, J. Xu, J. Fang, Z. Cao, L. Yang, and T. Li, "Potential for mine water disposal in coal seam goaf: investigation of storage coefficients in the Shendong mining area," *Journal of Cleaner Production*, vol. 244, no. C, p. 118646, 2020.

[34] L. Yang, J. Xu, J. Fang, Z. Cao, T. Li, and H. Song, "Risk evaluation of groundwater leakage in coal seam goaf: a case study in the Lingxin Mining Area," *Environmental Science and Pollution Research International*, vol. 27, no. 21, pp. 26066–26078, 2020.

[35] Q. Wang, W. Li, T. Li, X. Li, and S. Liu, "Goaf water storage and utilization in arid regions of Northwest China: a case study

of Shennan coal mine district," *Journal of Cleaner Production*, vol. 202, pp. 33–44, 2018.

[36] L. Zhao, C. Sun, P. Yan et al., "Dynamic changes of nitrogen and dissolved organic matter during the transport of mine water in a coal mine underground reservoir: column experiments," *Journal of Contaminant Hydrology*, vol. 223, article 103473, 2019.

[37] X. S. Kong, Z. Z. Xu, R. L. Shan, S. Liu, and S. C. Xiao, "Investigation on groove depth of artificial dam of underground reservoir in coal mines," *Environmental Earth Sciences*, vol. 80, no. 6, pp. 1–17, 2021.